REPORT DOCUMENTATION PAGE

Form Approved
OMB No. 0704-0188

1. REPORT DATE *(DD-MM-YYYY)*	2. REPORT TYPE	3. DATES COVERED *(From - To)*
07-Mar-2007	CONFERENCE PAPER	20 Sep 2006 - 22 Sep 2006

4. TITLE AND SUBTITLE

New Results Using Polyomino-Tiled Subarrays for Time-Delay Control of Wideband Arrays

5a. CONTRACT NUMBER
IN-HOUSE

5b. GRANT NUMBER
N/A

5c. PROGRAM ELEMENT NUMBER
61102F

6. AUTHOR(S)

R. J. Mailloux, S.G. Santarelli and T.M. Roberts

5d. PROJECT NUMBER
2304

5e. TASK NUMBER
HA

5f. WORK UNIT NUMBER
01

7. PERFORMING ORGANIZATION NAME(S) AND ADDRESS(ES)
AFRL/SNHA
Air Force Research Laboratory
80 Scott Drive
Hanscom AFB MA

8. PERFORMING ORGANIZATION REPORT

9. SPONSORING / MONITORING AGENCY NAME(S) AND ADDRESS(ES)
Electromagnetics Technology Division SOURCE CODE: 437890
Sensors Directorate
Air Force Research Laboratory
80 Scott Drive
Hanscom AFB MA 01731-2909

10. SPONSOR/MONITOR'S ACRONYM(S)
AFRL-SN-HS

11. SPONSOR/MONITOR'S REPORT NUMBER(S)
AFRL-SN-HS-TP-2006-0951

12. DISTRIBUTION / AVAILABILITY STATEMENT
APPROVED FOR PUBLIC RELEASE; DISTRIBUTION UNLIMITED; ESC 06-0951, DATE: 24 AUG 2006

13. SUPPLEMENTARY NOTES
Published in Proceedings of the 2006 Antenna Applications Symposium, Monticello, Illinois, 20 September 2006, p 188-202

14. ABSTRACT

This paper presents recent results describing the use of polyomino subarrays to introduce time delays into phased-array systems. Results for arrays of 8-element subarrays show suppression of peak quantization lobes to levels below -14 dB, relative to the quantization lobes of 8-element rectangular subarrays. Since algorithms for producing arbitrarily large arrays that tile rectangular areas are not available, we have combined smaller arrays chosen to be statistically independent. These have allowed the evaluation of ensemble averages of array gain, average and peak sidelobe levels.

15. SUBJECT TERMS
Antennas, phased arrays, subarrays, polyominos, wideband arrays

16. SECURITY CLASSIFICATION OF:			17.LIMITATION OF ABSTRACT	18.NUMBER OF PAGES	19a. NAME OF RESPONSIBLE PERSON
a. REPORT	b. ABSTRACT	c. THIS PAGE			Scott G. Santarelli
Unclassified	Unclassified	Unclassified	UU	17	19b. TELEPHONE NUMBER *(include area code)* N/A

Standard Form 298 (Rev. 8-98)
Prescribed by ANSI Std. Z39.18

NEW RESULTS USING POLYOMINO-TILED SUBARRAYS FOR TIME-DELAY CONTROL OF WIDEBAND ARRAYS

*R. J. Mailloux, **S. G. Santarelli, and **T. M. Roberts

* Department of Electrical and Computer Engineering, University of Massachusetts, Amherst Massachusetts
** Sensors Directorate, Air Force Research Laboratory
Hanscom, AFB, Massachusetts

Abstract: This paper presents recent results describing the use of polyomino subarrays to introduce time delays into phased-array systems. Results for arrays of 8-element subarrays show suppression of peak quantization lobes to levels below -14 dB, relative to the quantization lobes of 8-element rectangular subarrays. Since algorithms for producing arbitrarily large arrays that tile rectangular areas are not available, we have combined smaller arrays chosen to be statistically independent. These have allowed the evaluation of ensemble averages of array gain, average and peak sidelobe levels.

1. Introduction

Time delay is most often introduced into phased-array systems by using phase shifters at the array face and time-delay units behind rectangular subarrays. As discussed in many texts and publications, this practice leads to significant quantization lobes in the radiated pattern. The locations of these quantization lobes in angle space correspond to the grating lobes one would see for an array with inter-element spacing equal to the subarray dimensions. Obviously, quantization lobes represent severe pattern degradation.

Various subarray techniques have been developed to reduce quantization lobes. These methods, which include interlacing or overlapping the subarrays, have been understood for years [1, 2] and have been demonstrated in practice; however, these approaches are relatively difficult and expensive to build. In addition, thinned array techniques may be used, but they can have significant residual "error sidelobes" even at center frequency.

In addition to earlier symposium presentations by the present authors, there have been several other recent papers describing the use of random or irregular subarrays or other techniques for randomizing the phase-center locations of the subarrays [3-6]. In this paper, we show that the use of irregular-shaped subarrays can provide suppression of quantization lobes and that the subarrays can be realized entirely in the control network that feeds the elements.

2. Polyomino Subarrays

This paper describes a practical technique for using polyomino-shaped subarrays to provide time delay for a large array. Polyominos are figures composed of elements on a square grid. Systematic study of polyominos, as the general figures are named, began in 1953 and now has a substantial literature in mathematical combinatorics [7-10]. Particular L-shaped tetromino and octomino subarrays seem practical for reasons mentioned in the introduction and the earlier publications [3, 4]. The words tetromino and octomino are an extrapolation of the familiar word domino. Dominos have 2 elements; tetrominos have 4; and octominos have 8.

There have been numerous publications in mathematical journals dealing with the perfect 'tiling' of rectangular areas using various similar or dissimilar polyominos. "Perfect" implies that the rectangular area is completely filled such that no part of any polyomino extends beyond the rectangular boundary. In our application, however, we are dealing with a rectangular grid of array elements. Thus, we do not worry about having the tiles end exactly at the edges, since we can choose to either load these edge elements or simply not excite them. The few that extend beyond the edges, as in Figure 1 (with data shown in Figure 2) are of little concern for a large array. (The results shown later in Figures 6 and 7 are computed with an available tiling program that produces perfect tiling).

All of the polyomino arrays discussed in this paper adhere to the following rules:

1. Each array is tiled with a single polyomino shape. This shape may be rotated through 90° increments and is sometimes allowed to flip. Therefore, if we allow the polyomino to flip, there are a total of 8 different subarray configurations, as illustrated in Figure 1.
2. We require that the aperture be completely 'tiled' or filled with subarrays, with no gaps. In this manner, the center-frequency pattern will be identical to the center-frequency pattern of the phase-shifted array, and there will be no reduction in aperture efficiency.
3. We choose the number of elements in each subarray to be 2^n (for positive n), such that a lossless power divider can be used to feed each subarray.

All results discussed in this paper are for the L-octomino and the corresponding rectangular subarrays they replace. Figure 1 shows an array of 2048 (64 x 32) elements grouped into 256 L-octomino subarrays.

Working by hand, we were unable to perfectly tile any large array using octominos, so all of our hand-made tilings have elements protruding beyond the rectangular boundaries of the array [3]. These hand-made arrays resulted in some of the lowest-sidelobe designs; however, they were extremely tedious to construct. Fortunately, the literature offers computer programs that perfectly tile rectangular areas [7-10]. During the course of this

project, we have generated tens of millions of tilings using [9], which came to our attention as a Linux screensaver.

For a rectangular array of equal but rotated polyomino shapes, one can envision using a single type of power-divider network. There is no need to assemble the subarrays and place them into the array individually, or to design the array with mechanical structures that separate the subarrays, because the subarrays will be formed entirely in the control network that feeds the elements.

The array of L-octominos shown in Figure 1 was analyzed assuming that an amplitude taper was imposed at every element across the array, not just at the subarray ports. Parenthetically, we note that subarray amplitude quantization effects are usually much smaller than phase or time-delay quantization effects, especially in a large array; thus, we haven't studied them here.

The elements of each subarray are excited by a time-delayed signal, such that the time delay is exact for one of the elements (denoted as the phase-center element). Note that the phase-center element is the same for all 90° rotations of the subarray (both flipped and non-flipped). The phase shifters at the remaining elements in the subarray are chosen to produce a progressive phase across the subarray, and thus, a continuous phase progression across the entire array at center frequency.

The arrays are assumed to lie in the (x, y) plane of a spherical coordinate system radiating into the half space $z \geq 0$. Figure 2 shows pattern data plotted in direction cosine space ($u = \sin\theta\cos\phi$ and $v = \sin\theta\sin\phi$) for two arrays scanned to (u_0, v_0) = (0.5, 0.5). The first array has 256 rectangular subarrays of eight elements arranged in a 4 x 2 grid. The second array consists of 256 L-shaped octomino subarrays. The elements in both arrays are spaced 0.5 λ apart at the highest frequency, $r = f / f_0 = 1.2$.

Figure 2a shows the periodic quantization lobes for the rectangular case. Figure 2b shows the pattern corresponding to the array of L-shaped octomino subarrays depicted in Figure 1. Figures 2c and 2d show the three dimensional patterns (2a and 2b, respectively) projected onto a plane so that sidelobe levels can be measured. For the array of rectangular subarrays, the largest quantization lobe is approximately –11.5 dB below the broadside gain (Figure 2c). Results in Figure 2d for the array of octomino subarrays show lower peak sidelobes with the highest being approximately –25.9 dB relative to broadside gain, or reduced by approximately –14.4 dB relative to the rectangular subarray configuration. It should be noted that the difference in gain between the rectangular and octomino patterns is 0.1 dB based on pattern integration.

3. Dot-Product Metric

One of the goals of this project is to investigate peak and average sidelobe behavior as a function of array size; however, the tiling program that is used to generate the octomino

subarray configurations is limited to 32 x 32-element arrays. In order to generate larger arrays, we can combine any number of 32 x 32-element "unit cells." For example, two adjacent unit cells form a 32 x 64 array, whereas four unit cells can be used to generate a 64 x 64 array, as illustrated in Figure 3.

When generating these larger arrays, however, the unit cells must be chosen such that the tilings are significantly "different" from one another. For example, consider a 64 x 64-element array (like the one shown in Figure 3), which consists of 4 unit cells. If the unit cells are identical, or nearly identical, then this periodicity will manifest as quantization lobes in the radiated pattern. If the unit cells are chosen such that the tilings are significantly different, however, the corresponding quantization lobes are suppressed.

In order to measure the "degree of similarity" between any two unit cells, we applied the *dot-product metric*. This metric is implemented in neural network theory for pattern classification problems [11]. Basically, each pattern (i.e., unit cell) is represented as a multi-dimensional vector. The angle between any two vectors (i.e., patterns) **A** and **B** can be computed using the following:

$$\theta_{AB} = \cos^{-1}\left[\frac{\vec{A} \bullet \vec{B}}{\|\vec{A}\|\|\vec{B}\|}\right]. \qquad (1)$$

Smaller values of θ correspond to patterns that have a high degree of similarity, whereas larger values of θ indicate dissimilar patterns.

To illustrate this point, consider the pattern classification problem of Figure 4. Here, a 3 x 5 grid is used to represent numerical values from 0 to 9 by blackening the appropriate blocks. The pattern which represents the number zero is shown at the top of the figure. If we assign each black box a value of -1 and each white box a value of 1, we can describe this pattern in vector format (by taking the values column-wise) as follows: V_0 = [-1, -1, -1, -1, -1, -1, 1, 1, 1, -1, -1, -1, -1, -1, -1]. The patterns representing the numerals one and eight are shown at the bottom of the figure. Applying equation (1), it can be shown that the dot-product angle between patterns zero and one, θ_{01}, is 137.2°, whereas θ_{08} is only 29.9°. These results are expected, since the "zero" pattern is very similar to the "eight" pattern (i.e., differs by only a single block-value), whereas the "zero" pattern is quite dissimilar to the "one" pattern (i.e., the two patterns have only two blocks in common).

For this project, we tile a unit cell using a single octomino shape, namely, the L-shaped octomino. There exist eight orientations for this octomino as shown in Figure 5. Each orientation is assigned a unique bipolar, binary representation; thus, every element within

a particular octomino is assigned the same binary number. Again, taking the array elements column-wise, a 384-element vector is formed (i.e., 128 octominos x 3-bit representation) for each unit cell. When the unit cell shown at the top of the figure is compared to the unit cell directly below, we see that the dot-product angle is only 10.1°. This result is expected, since these two unit cells differ only in the small area indicated by the circles; otherwise, these two tilings are identical. On the other hand, the dot-product angle between the top unit cell and the bottom-right unit cell is much larger, indicating that the two patterns are dissimilar, and this dissimilarity is easily recognized by a simple visual comparison.

4. Statistics for octomino unit-cell arrays and arrays of unit cells

Using the polyomino tiling program described in [9], we generated 99 random tilings of L-shaped octominos. Each tiling consisted of 128 octominos and covered an area corresponding to a 32 x 32-element array or "unit cell" (as previously defined and as shown in Figure 3). We subsequently measured the dot-product angle, θ, between each unit cell and every other one (i.e., $0.5 \times 99 \times 98 = 4{,}851$ dot-product computations). The values for θ ranged from roughly 75° to 105°, indicating that there is a fairly high degree of dissimilarity across the entire set of tilings. As mentioned previously, it is desirable to use dissimilar unit cells when constructing larger arrays, since unwanted periodicities in the array structure often manifest as large quantization lobes in the radiated pattern.

We used 96 unit cells to construct twenty-four 64 × 64 arrays. Then, we calculated the radiation pattern for each of the original ninety-nine 32 × 32 arrays in addition to the newly constructed 64 × 64 arrays. Figure 6 shows the average sidelobe levels for both sets of tilings as a function of frequency. The x-axis represents the ratio $r = f / f_0$, where f_0 denotes center frequency. The y-axis represents amplitude in decibels. The average sidelobe levels for the entire set of 32 × 32 *octomino* arrays are plotted vertically for each value of r. The small blue dots represent the individual values, whereas the large blue circle indicates the mean value at each frequency point. The average sidelobe level of the corresponding 32 × 32 *rectangular* array (which consists of a grid of 128, 2 × 4-element subarrays) is also plotted as a function of r (red solid line) for comparison.

Similarly, the average sidelobe levels for the entire set of 64 × 64 *octomino* arrays are plotted as a function of r denoted by blue triangles, and the corresponding 64 × 64 *rectangular* array (which consists of a grid of 256, 2 × 4-element subarrays) is also plotted as a function of r (red dotted line).

As expected, there is a general trend for the average sidelobe level to increase as f departs from center frequency. It is also apparent that, for a given array size, the octomino curve tracks the corresponding rectangular curve rather closely. In most cases, there is less than 1 dB difference between the mean value of the octomino curve and the corresponding rectangular curve; however, the octomino curve tends to lie above the rectangular curve for almost all values of r. Thus, we can conclude that although the octomino array

structure is able to suppress the quantization lobes that manifest from the periodic structure of the rectangular array, the random phase errors introduced by the octomino array structure cause the average sidelobes to increase slightly.

If we look closely at the octomino curves for either array size (i.e., 32 × 32 or 64 × 64), it is evident that for each value of r, the individual values vary from the mean by roughly 1 dB or less. This implies that the average sidelobe level does not change significantly as a function of array tiling. On the other hand, the difference between curves corresponding to different array sizes (i.e., the difference between the two rectangular curves or the difference between the two octomino curves) is a fairly constant 5 – 6 dB. This result is not surprising, since one would expect the average sidelobe level to be inversely proportional to the array size (i.e., the average sidelobe level itself is proportional to the phase-error variance and is independent of the array size, so doubling the array size reduces the average level by about 6 dB).

Figure 7 plots maximum sidelobe level as a function of tiling configuration for the set of 64 × 64 octomino arrays for a constant frequency ratio of $r = 0.7$. The solid red line represents the maximum sidelobe level for the corresponding 64 × 64 rectangular array. Note that even the worst of the octomino arrays (tiling #2) is roughly 8 – 9 dB below the rectangular value, and some of the octomino arrays (tilings #4 and #24) are as much as 15 dB below the rectangular value. Thus, the range of values is considerable – roughly 6.5 dB. Overall, these results suggest that, although the *average* sidelobe level does not depend heavily on tiling configuration, the *maximum* sidelobe level does. In addition, this wide range of values corresponding to the maximum sidelobe level illustrates the importance of array simulation and analysis as part of the design process. For example, the analysis presented in Figure 7 allows one to choose a "good" tiling (such as #4 or #24) rather than a "bad" tiling (such as #2). As a final note, the peak sidelobe performance of any given tiling varies very little with frequency, as illustrated in Figure 8. Here we see that tilings #4 and #24 consistently outperform tiling #2 at every frequency (except, of course, at center frequency where all three tilings become equivalent to the rectangular case).

5. Conclusion

This study has presented data from arrays of L-octomino shaped subarrays used to provide time-delay steering for a phase-steered array. The paper demonstrates elimination of the -11.5 dB quantization lobes that are radiated by an array of rectangular subarrays, and their replacement by lower sidelobes that are between –25 and –26 dB below the main-beam gain.

Acknowledgements: This work was supported by the Air Force Office of Scientific Research, Mathematics and Space Sciences Directorate, under Dr. A. Nachman.

References:

[1] R. Tang, "Survey of time delayed beam steering techniques," in Phased Array Antennas: Proc. of the 1970 Phased Array Antenna Symposium, Artech House, Dedham, MA 1972, pp. 254-260.

[2] R. J. Mailloux, Phased Array Antenna Handbook, 2nd Edition, Artech House Publishing Co., Dedham, MA, 2005.

[3] R. J. Mailloux, S. G. Santarelli, T. M. Roberts, "Irregular shaped subarrays for time delay control of planar arrays," Proceedings of the 2004 Antenna Applications Symposium, Monticello, Illinois.

[4] R. J. Mailloux, S. G. Santarelli, T. M. Roberts, "Polyomino shaped subarrays for limited field of view and time delay control of planar arrays," Proceedings of the 2005 Antenna Applications Symposium, Monticello, Illinois.

[5] R. C. Hansen, and G. G. Charlton, "Subarray Quantization Lobe Decollimation," IEEE Trans. AP-47, No.8, August 1999, pp.1237-1239.

[6] V. Pierro, V. Galdi, G. Castaldi, I. M. Pinto, and L. B. Felson, " Radiation properties of planar antenna arrays based on certain categories of aperiodic tilings," IEEE Trans. AP-53, No.2, February 2005, pp. 635-643.

[7] S. W. Golomb, Polyominoes: Puzzles, Patterns, Problems, and Packings, Princeton University Press, Princeton, New Jersey, 2nd edn., 1994.

[8] G. E. Martin, Polyominoes: A Guide to Puzzles and Problems in Tiling, Mathematical Association of America, Washington, DC, 1991.

[9] S. Montgomery-Smith, "\polyomino-0.4," available online http://www.math.missouri.edu/_stephen/software/polyomino.

[10] G. Putter, "\Gerard's Universal Polyomino Solver," available online http://www.xs4all.nl/_gp/PolyominoSolver/Polyomino.html.

[11] M. T. Hagan, H. B. Demuth, M. H. Beale, Neural Network Design, Martin Hagan Publishing, 2002.

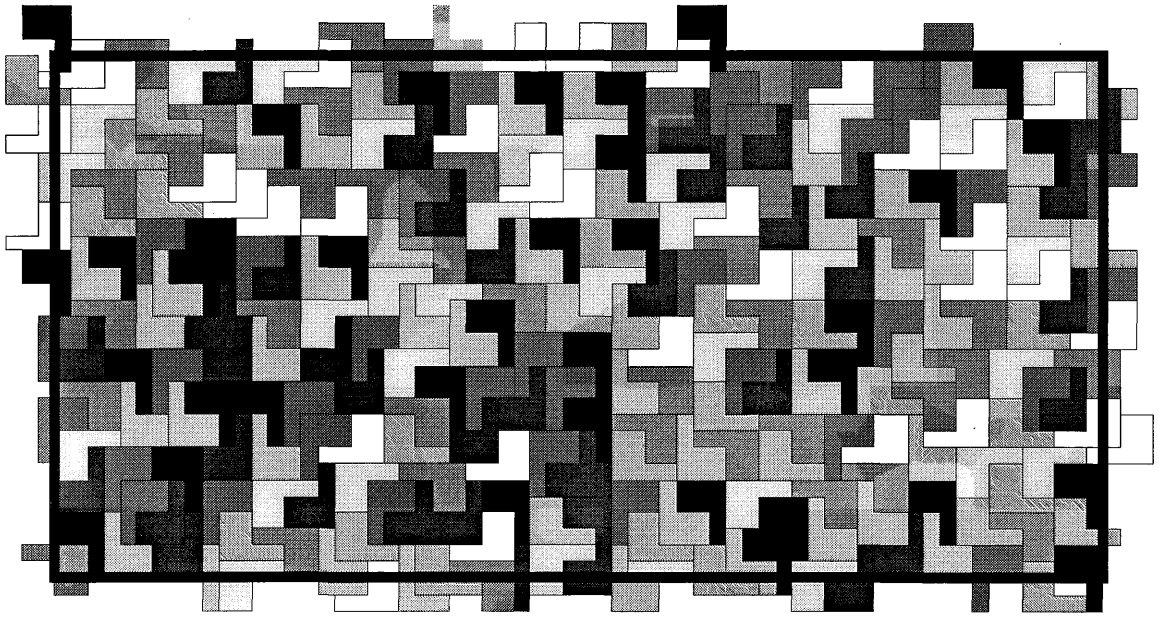

Figure 1. Array of 2048 elements consisting of 256 L-octomino subarrays).

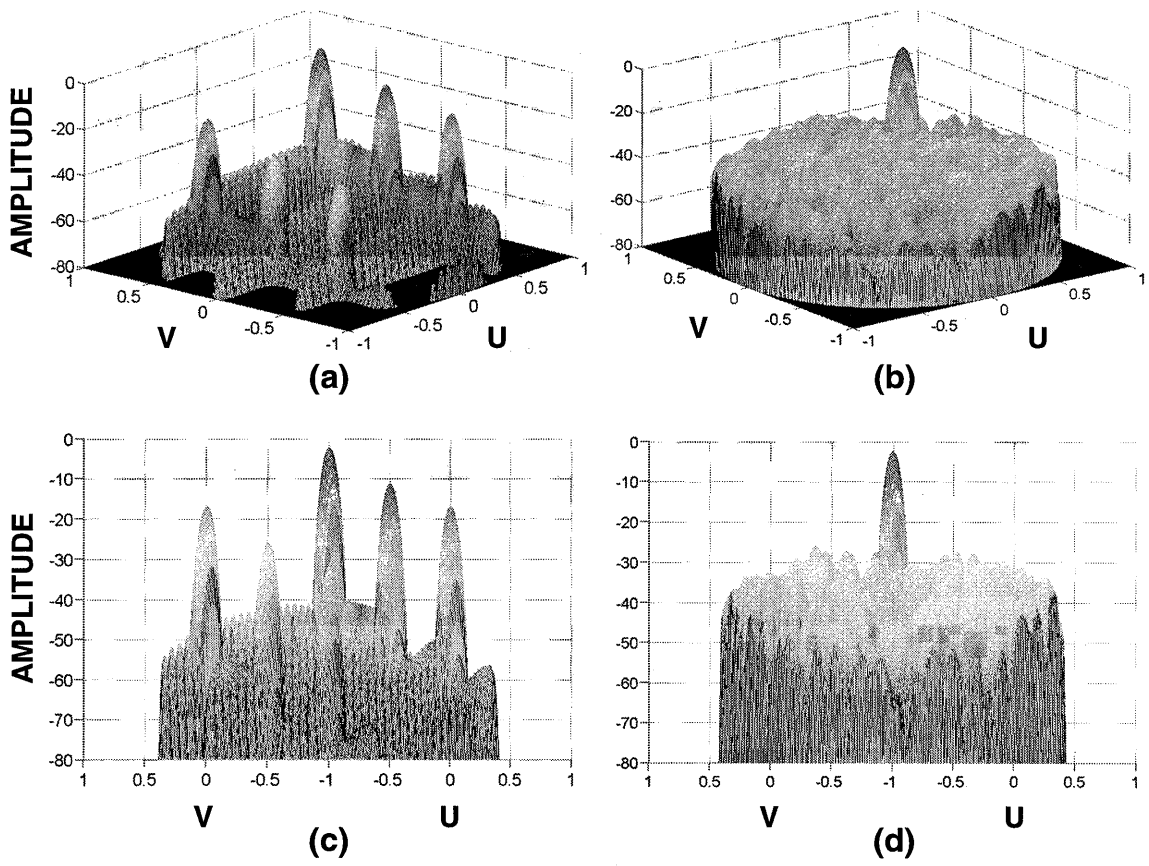

Figure 2. 3-D sidelobe profiles for arrays of rectangular and polyomino subarrays at a scanning angle of $(u_0,v_0) = (0.5,0.5)$. (a) Array pattern of rectangular (2 x 4) subarrays. (b) Array pattern of L-octomino subarrays. (c) Projected pattern of rectangular subarrays. (d) Projected pattern of L-octomino subarrays.

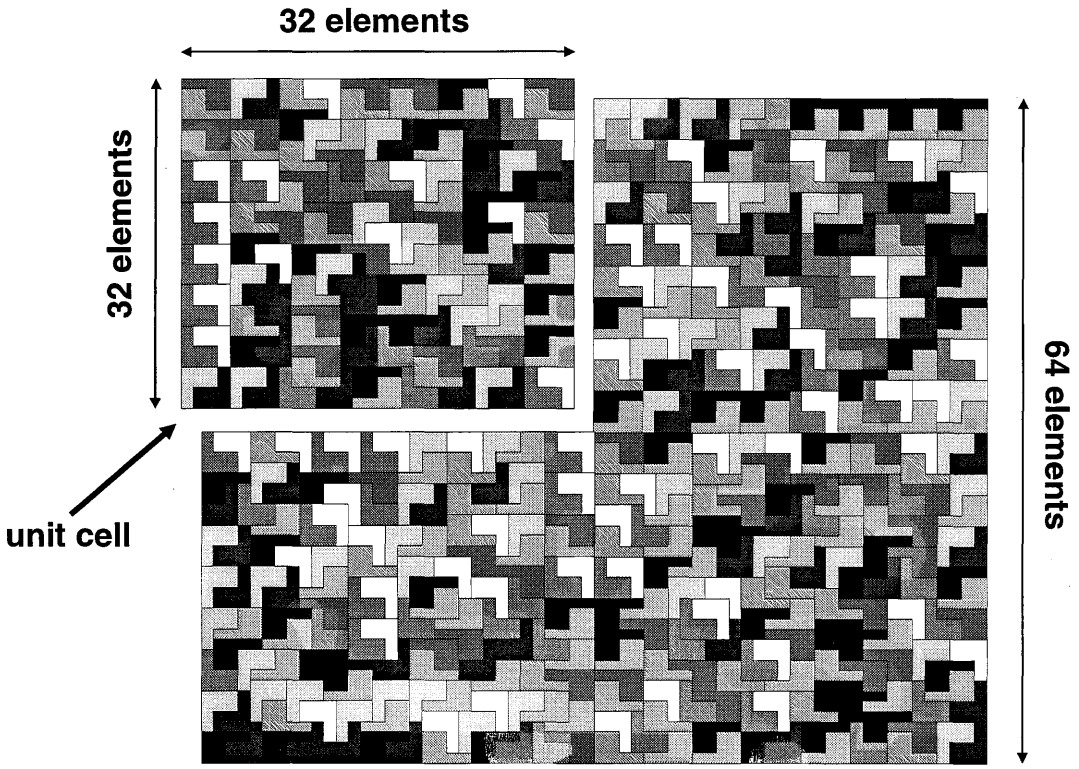

Figure 3. Definition of a "unit cell".

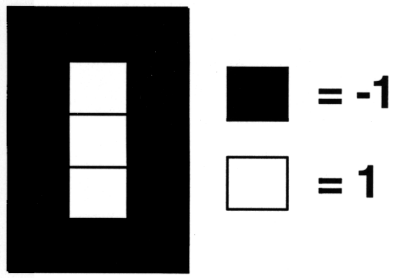

$V_0 = [-1, -1, -1, -1, -1, -1, 1, 1, 1, -1, -1, -1, -1, -1, -1]$

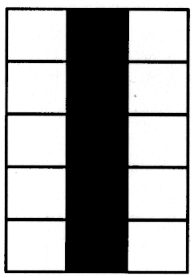

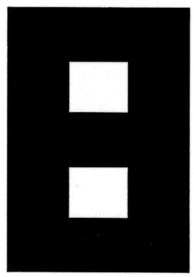

$\theta_{01} = 137.2°$

$\theta_{08} = 29.9°$

Figure 4. Dot-product metric example.

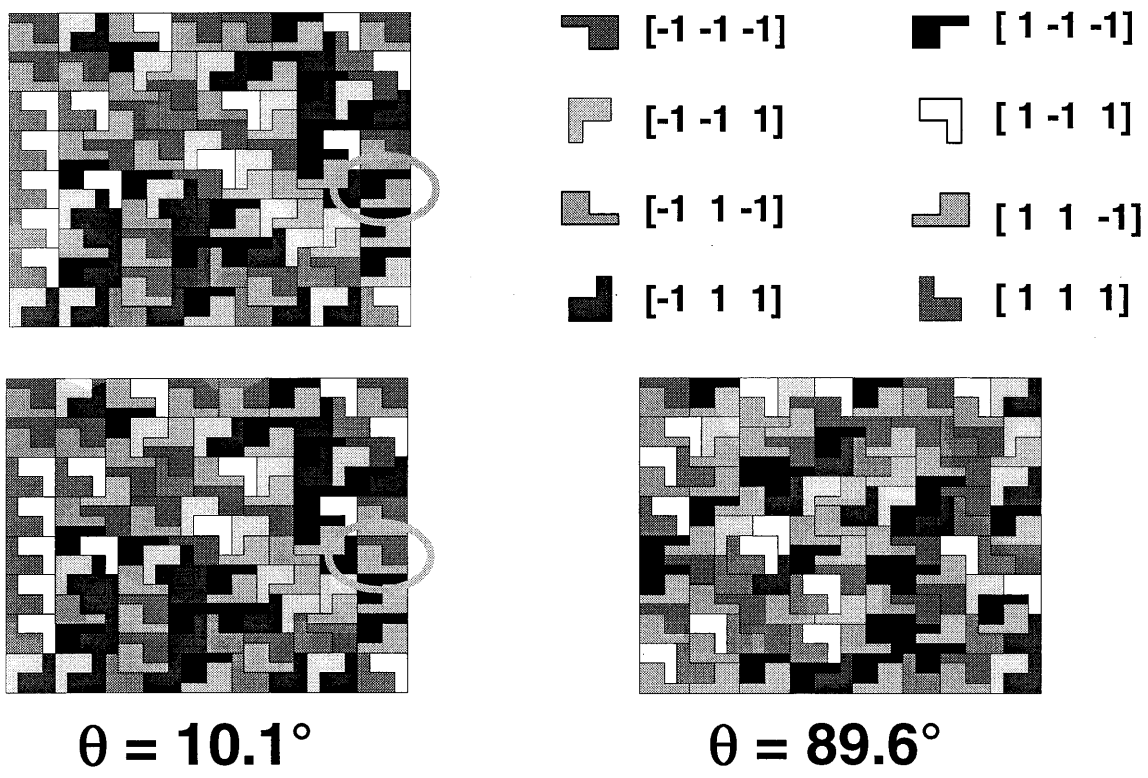

Figure 5. Dot-product metric applied to unit cells.

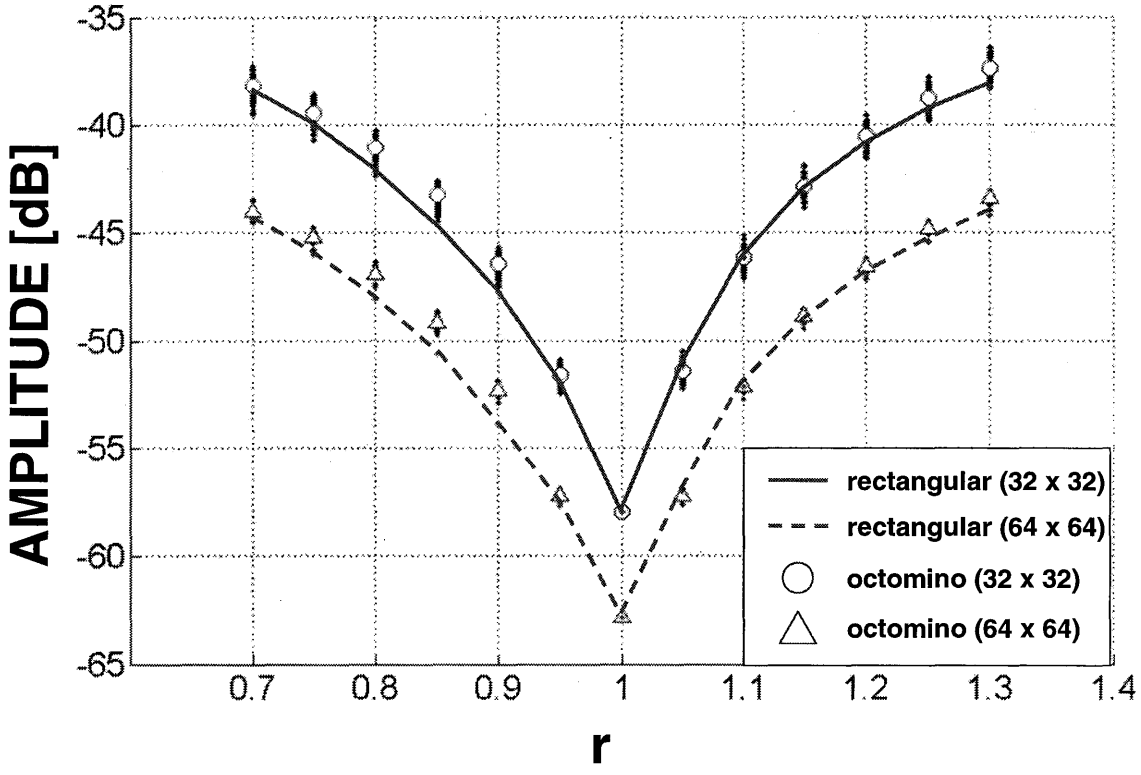

Figure 6. Statistical analysis of average sidelobe levels as a function of frequency for two array sizes: 32 x 32 and 64 x 64.

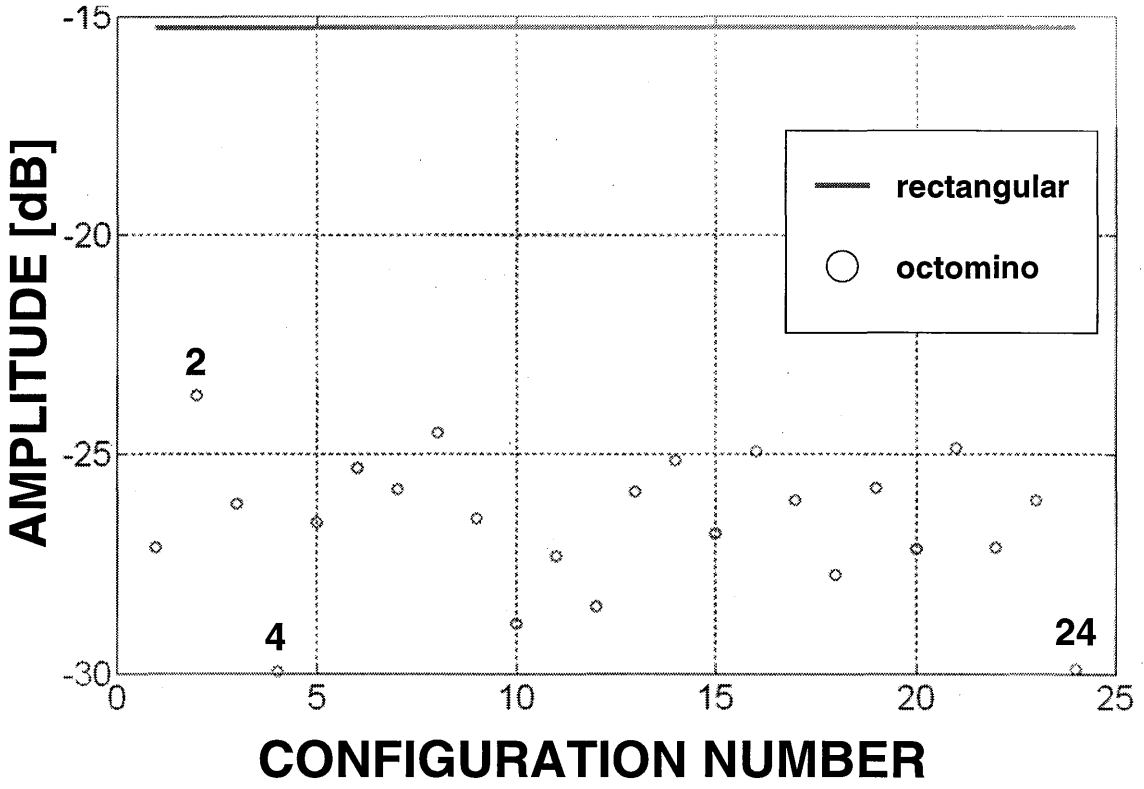

Figure 7. Comparison of maximum sidelobe level for rectangular (solid) and octomino (circles) arrays for $r = 0.7$.

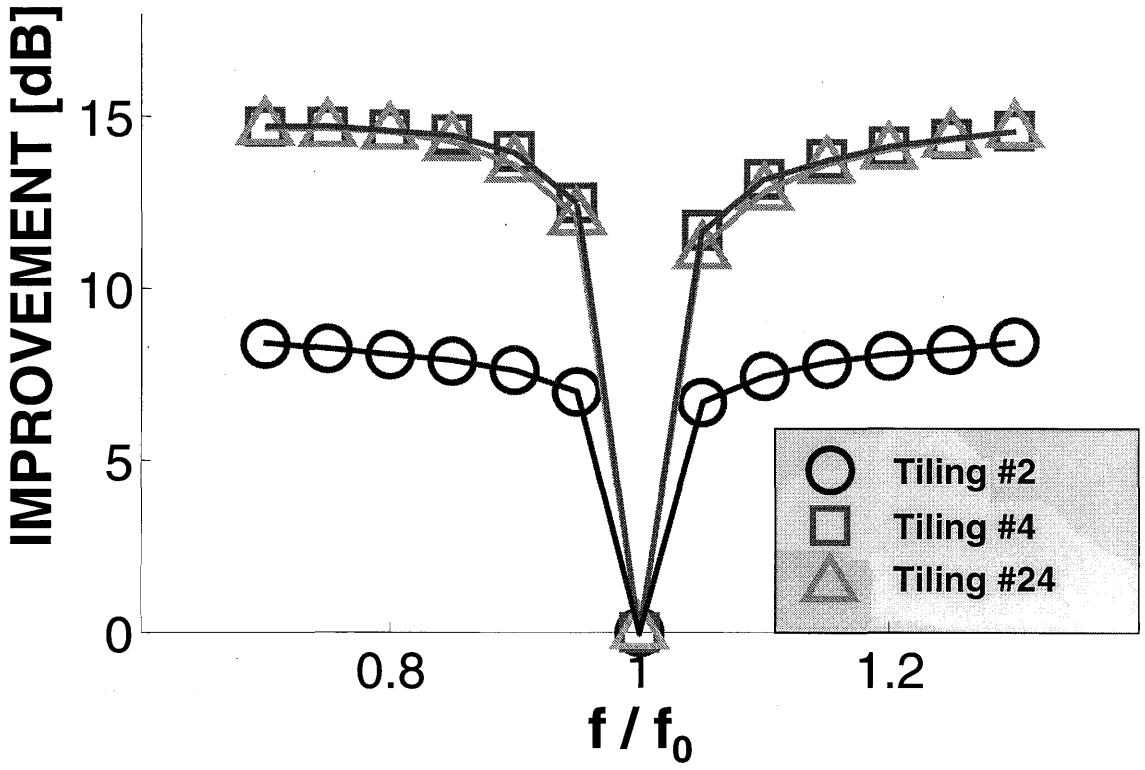

Figure 8. Peak sidelobe level (normalized to rectangular case) as a function of frequency for tilings #2 (circle), #4 (square), and #24 (triangle) of Figure 7.